Motion corrected photoacoustic difference imaging of fluorescent contrast agents

Julia Märk[*a], Asja Wagener[b], Sarah Pönick[b], Carsten Grötzinger[b], Edward Zhang[c], Jan Laufer[a,d]

[a]Institute of Optics and Atomic Physics, Technische Universität Berlin, Straße des 17. Juni 135, Berlin, Germany
[b]Department of Gastroenterology and Hepatology, Charité University Hospital, Charitéplatz 1, Berlin, Germany
[c]Department of Medical Physics and Bioengineering, University College London, Gower Street, London WC1E 6BT, UK
[d]Institute of Radiology, Charité University Hospital, Charitéplatz 1, Berlin, Germany

ABSTRACT

In fluorophores, such as exogenous dyes and genetically expressed proteins, the excited state lifetime can be modulated using pump-probe excitation at wavelengths corresponding to the absorption and fluorescence spectra. Simultaneous pump-probe pulses induce stimulated emission (SE) which, in turn, modulates the thermalized energy, and hence the photoacoustic (PA) signal amplitude. For time-delayed pulses, by contrast, SE is suppressed. Since this is not observed in endogenous chromophores, the location of the fluorophore can be determined by subtracting images acquired using simultaneous and time-delayed pump-probe excitation. This simple experimental approach exploits a fluorophore-specific contrast mechanism, and has the potential to enable deep-tissue molecular imaging at fluences below the MPE. In this study, some of the challenges to its *in vivo* implementation are addressed. First, the PA signal amplitude generated in fluorophores *in vivo* is often much smaller than that in blood. Second, tissue motion can give rise to artifacts that correspond to endogenous chromophores in the difference image. This would not allow the unambiguous detection of fluorophores. A method to suppress motion artifacts based on fast switching between simultaneous and time-delayed pump-probe excitation was developed. This enables the acquisition of PA signals using the two excitation modes with minimal time delay (20 ms), thus minimizing the effects of tissue motion. The feasibility of this method is demonstrated by visualizing a fluorophore (Atto680) in tissue phantoms, which were moved during the image acquisition to mimic tissue motion.

Keywords: stimulated emission, fluorophore, photoacoustic imaging, pump-probe measurements, motion correction

*julia.maerk@tu-berlin.de

1. INTRODUCTION

Photoacoustic imaging (PAI) allows the noninvasive visualization of tissue absorbers with scalable spatial resolution to cm depths, and has the potential for functional and molecular imaging[1]. Whilst fluorophores have been used as contrast agents in PAI in proof-of-principle studies to demonstrate visualization *in vivo* at greater depths and with higher spatial resolution than that provided by purely optical modalities[2], their unambiguous detection remains challenging. A wide field of potential applications has also recently been opened by the development of new genetically expressed fluorescent proteins that provide absorption in the near-infrared spectral region where the optical tissue penetration depth is greatest[3–6]. However, to determine the spatial distribution of tissue chromophores and fluorescent contrast agents, approaches, which involve the acquisition of multiwavelength images and the subsequent application of spectral unmixing methods, such as model-based inversion schemes[7,8], are typically used. The challenges of this approach are that (i) it is computationally expensive, (ii) it relies upon accurate prior information on all tissue chromophores, such as their absorption spectra and PA properties[9], and (iii) the wavelength dependent fluence attenuation inside the tissue needs to be accounted for. For the detection of fluorophores, the validity of multispectral unmixing methods is

Photons Plus Ultrasound: Imaging and Sensing 2016, edited by Alexander A. Oraevsky, Lihong V. Wang
Proc. of SPIE Vol. 9708, 970821 · © 2016 SPIE · CCC code: 1605-7422/16/$18 · doi: 10.1117/12.2207302

compromised by fluence dependent deviations in the absorption and thermalization properties, which are due to the typically long excited state lifetimes[10], from those presumed known *a priori*.
In a previous study, we presented an alternative, experimental method for the detection of fluorophores that has the potential to overcome these limitations. It is based on the generation of PA signals using pump-probe excitation that exploits stimulated emission to induce fluorophore specific contrast in difference images[11]. Furthermore, it allows visualizing differences in the excited state lifetime[12], which may find applications in sensing environmental parameters and as a contrast mechanism for multiplexing. While the pump-probe imaging method was validated theoretically and experimentally in tissue phantoms[13], there are two challenges to its application *in vivo*: (i) PA signals generated in fluorophores *in vivo* are often much smaller than those in blood, and (ii) tissue motion, e.g. related to breathing or heartbeat, can give rise to artifacts in the difference image that correspond to the movement of non-fluorescent absorbers and therefore impede the unambiguous detection of fluorophores. In this study, we adapted the experimental pump-probe method in order to reduce motion artifacts by using a fast acquisition of PA difference signals. The new method is validated by imaging fluorophores in a non-stationary tissue phantom.

2. BACKGROUND

2.1 PA signal generation in fluorophores

After absorbing a photon, non-fluorescent tissue chromophores (such as Hb, water and lipids) quickly relax back to the ground state (within ps) due to very short excited state lifetimes. The entire optical energy of the photon is thermalized due to vibrational dissipation. By contrast, fluorescent molecules typically have long excited state lifetimes. Upon absorption of a pump photon, an electronically and vibrationally excited molecule first relaxes to the lowest vibrational level of the excited electronic state (within ps)[14]. It subsequently returns to the electronic ground state either via spontaneous emission of a photon, i.e. fluorescence, or via non-radiative processes, such as vibrational decay, internal conversion and inelastic collisions. The return to the ground state can be comparatively slow, occurring on time scales ranging from several hundred ps to several ns[15,16]. The different relaxation processes are competitive and only non-radiative relaxation contributes to the generation of the PA signal. The PA signal amplitude generated in fluorophores is reduced with respect to those generated in non-fluorescent chromophore solutions due to (i) the fluorescence emission according to the quantum yield and (ii) ground state depopulation that may occur during ns excitation pulses[17,10].

2.2 Excited state lifetime modulation of fluorophores with pump-probe excitation

Using a pump-probe excitation method we first introduced in [11], the excited state lifetime of fluorescent molecules can be modulated. The principle relies on adding a second, simultaneous probe pulse at the wavelength of fluorescence emission to accelerate the relaxation of the long-lived excited states by stimulated emission (SE)[18,19]. This causes a non-linear change in the amount of thermalized energy during the laser pulse and, hence, the PA signal of the fluorophore. The thermalization scheme of a fluorophore during pump-probe excitation is illustrated in Figure 1.

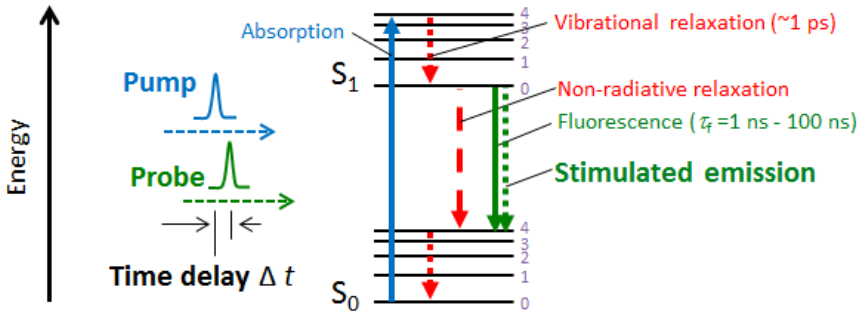

Figure 1. Schematic of the electronic and vibrational transitions in a fluorophore during pump-probe excitation (S0: electronic ground state, S1: first excited electronic state).

The efficiency of SE can be changed by introducing a time delay between pump and probe pulse. If the time delay is longer than the fluorescence lifetime of the fluorophore, SE is suppressed. By subtracting the PA signal obtained with delayed pump-probe excitation (without SE) from the signal obtained with simultaneous pump-probe excitation (with

SE), a distinct difference signal can be obtained. This can be exploited as a PA contrast mechanism, since the amplitude of signals generated in non-fluorescent, endogenous chromophores is not modulated by the pump-probe excitation (irrespective of time delay), and is therefore eliminated in the difference signals.

3. MATERIALS AND METHODS

3.1 Experimental Setup

A wavelength tunable OPO laser system (Newport, Spectra Physics, USA) provided pump and probe excitation pulses of 7 ns duration at a repetition frequency of 50 Hz. The signal and idler output of the OPO laser system were coupled into multimode fused silica fibers (1.5 mm core diameter) for mode scrambling and directed to an all-optical PA scanner[20]. For experiments, a fluorophore (Atto680) was used since its absorption and fluorescence spectra coincide with the signal and idler wavelengths provided by the OPO laser. Small portions of the excitation pulses were directed to an integrating sphere to measure the pulse energy with a wavelength calibrated photodiode/integrator system, and to measure the wavelength with an USB spectrometer (Ocean Optics, USA).

PA difference imaging was implemented using two methods. For Method A, a delay line on sliding stages was used to introduce a variable time delay Δt for the idler pulse to change the efficiency of SE. The imaging protocol involved the acquisition of two images using (1) simultaneous pump-probe excitation, and (2) delayed pump-probe excitation (by moving the rail to maximize Δt). A difference image was calculated by subtracting the images, i.e. (1) - (2). The drawback of this method is that it is strongly affected by tissue motion due to the sequential image acquisition as implemented by the current PA scanner, which results in image acquisition times of up to several minutes. To address this issue, Method B was developed. The rail-mounted delay line was replaced by a galvo, which was added to the idler beam path in order to couple the beam into either a 5 m or an 8 m length fused silica fiber, switching with each pulse. This allowed two PA signals to be recorded at each raster scan position using (1) simultaneous pulses and (2) time delayed pulses ($\Delta t \sim 15$ ns) at the laser pulse repetition frequency of 50 Hz. From the two PA signals a difference image was then calculated. Due to the short duration between the signal acquisitions at each scan point (20 ms), Method B minimizes motion artifacts.

3.2 PA difference imaging in tissue phantoms

Method A and B were compared by acquiring images in a tissue phantom while (i) keeping the phantom stationary and (ii) moving the phantom during the image acquisition to mimic tissue motion. The phantom consisted of polymer capillaries filled with either Atto680, a NIR fluorescence dye in methanol solution at a concentration of 75 µM (μ_a = 2.2 mm^{-1} at 680 nm, fluorescence lifetime τ_f = 2.7 ns) or copper chloride ($CuCl_2$) in aqueous solution at a concentration of 0.8 M (μ_a = 2.1 mm^{-1} at 742 nm) representing a stable absorber, immersed in a scattering lipid suspension ($\mu_s' \sim 1$ mm^{-1}). The pump fluence Φ_{pump} was 3.5 mJ/cm² (680 nm) and the probe fluence Φ_{probe} was 5 mJ/cm² (742nm). The phantom was placed on the PA scanner based on a Fabry-Perot polymer film ultrasound sensor[20] and image data sets were acquired using Method A and B. To mimic tissue motion, the phantom was translated by 1.5 mm in *y* during the measurement. For Method A, it was translated between the acquisition of the image with simultaneous pump-probe excitation and that with time-delayed pump-probe excitation. For Method B, it was translated during the image acquisition.

4. RESULTS

4.1 Pump-probe imaging of a stationary phantom

Both methods were tested by acquiring difference images of a stationary tissue phantom. Figure 2(a) and (b) show 2D cross sections of the images acquired using simultaneous pump-probe excitation, time delayed pump-probe excitation and the resulting difference image obtained using Method A (a) and Method B (b), respectively. In Figure 2(c), image intensity profiles (as indicated by the dashed lines in Figure 2(a)) across Atto680 and $CuCl_2$ filled tubes are shown.

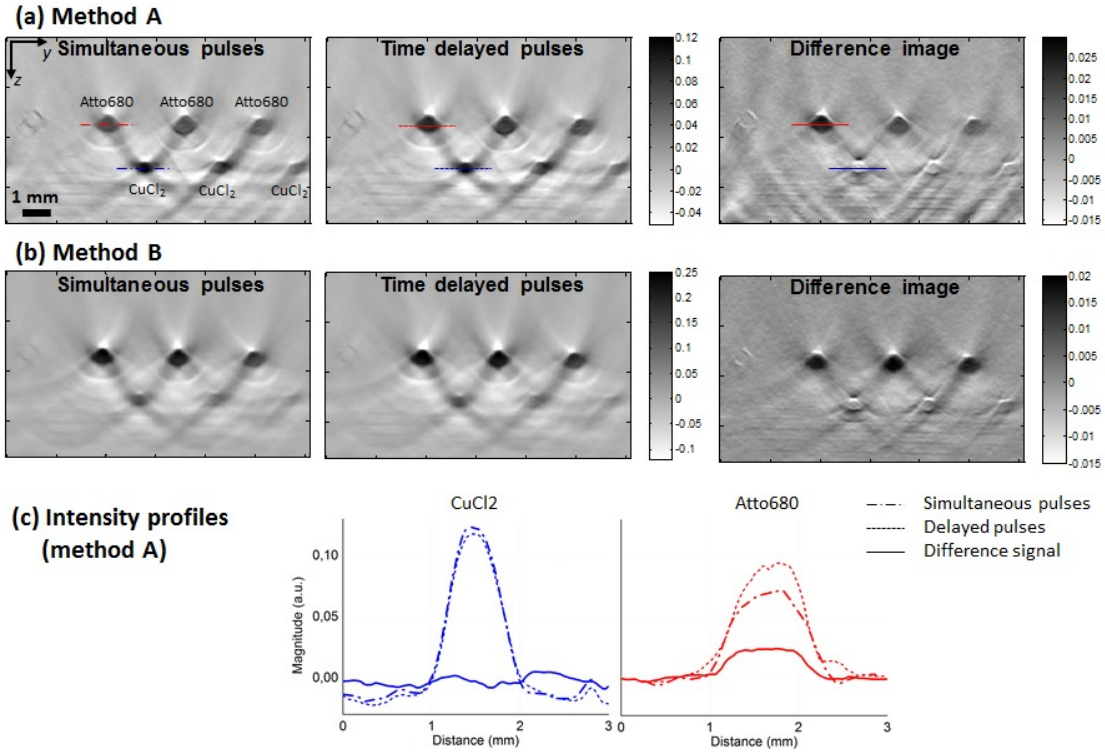

Figure 2. Difference imaging of a stationary tissue phantom consisting of polymer capillaries filled with Atto680 and $CuCl_2$. 2-D x-z cross sectional images of 3-D PA image data sets were acquired (a) without motion correction (Method A) and (b) with motion correction (Method B) using simultaneous and time delayed pump-probe pulses, and the calculated difference image. (c) Intensity profiles across the $CuCl_2$ and Atto680 tubes as indicated by dashes in (a).

For both methods, the Atto680 filled tubes are clearly visible in the difference image, while those from the $CuCl_2$ filled tubes are strongly reduced. Residual signals detected in the region corresponding to the $CuCl_2$ filled tubes may be attributed to weak polymer absorption, and shading effects originating from Atto680 filled tubes due to image reconstruction artifacts related to the limited field of view of the planar detection geometry. From the intensity profiles across the $CuCl_2$ tubes in Figure 1(c), no significant difference can be observed for simultaneous and time delayed pulses, and the difference signal corresponds to the noise floor. By contrast, for the Atto680 tube the signal increases for time delayed pulses without SE and the resulting difference signal has a SNR of ~ 25. The results obtained using Method A and B in a stationary phantom are therefore comparable.

4.2 Pump-probe imaging of a moving phantom

Method A and B were used to image a phantom which was translated laterally during the difference image acquisition. Figure 3(a) shows the 2D cross sections of the phantom images obtained using Method A for simultaneous pulses (position 1), for time delayed pulses following translation (position 2), and the resulting difference image. Figure 3(b) shows the cross sections of the phantom images obtained using Method B where the phantom was translated during the image acquisition (from left to right: for simultaneous pulses, for time delayed pulses, and the difference image). Figure 3(c) shows the image intensity profiles across Atto680 and $CuCl_2$ filled tubes in the difference image for Method A and B as indicated by dashed lines.

Without motion correction, the translation of the phantom during the measurement leads to strong difference signals for both types of absorber. In *in vivo* images, such artifacts could cause a false positive detection of a fluorophore. By contrast, motion correction strongly reduces the background signals from $CuCl_2$ filled tubes in the difference image, despite the movement of the phantom. While the location of the fluorophore appears blurred due to the motion, its presence is accurately detected and visualized in the difference image using Method B. The difference image intensities are also similar to those obtained in the stationary phantom. The residual difference image intensity corresponding to the $CuCl_2$ filled tubes is about three times lower than that of the Atto680 filled tubes.

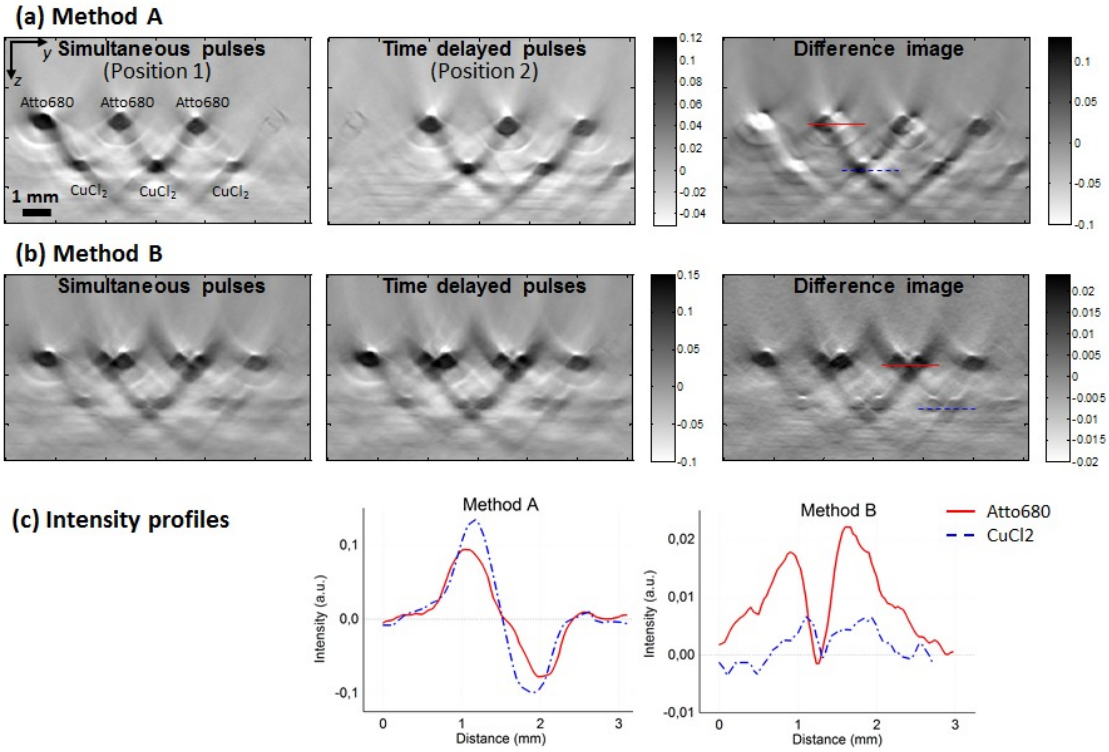

Figure 3. Difference imaging of a moving tissue phantom. 2-D x-z cross sectional images of 3-D PA image data sets acquired (a) without motion correction (Method A) and (b) with motion correction (Method B) using simultaneous and time delayed pump-probe pulses and the calculated difference image. (c) Intensity profiles across the $CuCl_2$ and Atto680 tubes in the difference images as indicated by dashes in (a) and (b), respectively.

5. DISCUSSION

Pump-probe excitation changes the PA signal amplitude of a fluorophore due to SE. The physical mechanism underlying this change is the reduction of the fluorescence lifetime by SE together with the associated change in fluorescence quantum yield. SE induces fast radiative transitions to the ground state from the otherwise long-lived excited states of fluorophores. For a single absorption-relaxation cycle during the excitation pulse, SE reduces the amount of thermalized energy. Using delayed pump-probe excitation with a probe pulse time delay exceeding the lifetime of the fluorophore, SE is suppressed. This mechanism was implemented in our experimental setup by introducing a time delay for the probe pulse either using a delay line or by fast switching between fibers of two different lengths using a galvo in order to reduce motion artefacts. By calculating difference images from data sets obtained using simultaneous and time-delayed excitation pulses, a fluorophore specific contrast is generated. This contrast mechanism provided a clear visualization of the fluorophore in difference images acquired in phantoms, while the signals generated in tubes filled with a non-fluorescent absorber were suppressed. The motion correction method using pulse-to-pulse switching between simultaneous and time delayed pump-probe excitation was shown to be much more effective in suppressing motion artifacts. Based on the fast acquisition of difference signals at every raster scan position with a minimal time delay of 20 ms, erroneous difference signals due to movements over larger time scales can be reduced. This presents a clear advantage in comparison to the difference imaging method that relies on the sequential acquisition of image data sets using a rail-mounted delay line. However, complete background suppression may also be compromised in some image regions due to for example fluence inhomogeneity, since the alignment of signal and idler beams transmitted by two separate multimode fibers could be optimized. The motion-corrected pump-probe imaging method proposed in this paper may enable the *in vivo* detection of fluorescent contrast agents in tomographic PA images even at low concentrations against the overwhelming contrast produced by endogenous tissue chromophores.

6. CONCLUSION

This study has demonstrated that a motion-corrected pump-probe excitation technique enables fluorophore detection in PA difference images in a moving tissue phantom. A method to suppress motion artifacts based on fast switching between simultaneous and time-delayed pump-probe excitation was developed. This enables the acquisition of PA signals using the two excitation modes with minimal time delay, thus minimizing the effects of tissue motion. The feasibility of this method is demonstrated by visualizing a NIR fluorophore in a tissue phantom, which was moved during image acquisition to mimic tissue motion. Using motion artifact suppression, this simple experimental approach exploiting a fluorophore-specific contrast mechanism has the potential to visualize the location of fluorophores in tomographic PA images and enable deep-tissue molecular imaging at fluences below the MPE. The method may be applied in *in vivo* applications, such as preclinical imaging of exogenous or genetically expressed fluorescent labels in small animal models of human disease.

ACKNOWLEDGEMENTS

This work was funded by ERC Starting Grant 281356.

REFERENCES

[1] Wang, L. V., Hu, S., "Photoacoustic Tomography: In Vivo Imaging from Organelles to Organs," Science **335**(6075), 1458–1462 (2012).

[2] Razansky, D., Vinegoni, C., Ntziachristos, V., "Multispectral photoacoustic imaging of fluorochromes in small animals," Opt. Lett. **32**(19), 2891–2893 (2007).

[3] Lecoq, J., Schnitzer, M. J., "An infrared fluorescent protein for deeper imaging," Nat. Biotechnol. **29**(8), 715–716, Nature Publishing Group (2011).

[4] Filonov, G. S., Piatkevich, K. D., Ting, L.-M., Zhang, J., Kim, K., Verkhusha, V. V., "Bright and stable near-infrared fluorescent protein for in vivo imaging," Nat. Biotechnol. **29**(8), 757–761 (2011).

[5] Razansky, D., Distel, M., Vinegoni, C., Ma, R., Perrimon, N., Köster, R. W., Ntziachristos, V., "Multispectral opto-acoustic tomography of deep-seated fluorescent proteins in vivo," Nat. Photonics **3**(7), 412–417 (2009).

[6] Krumholz, A., Shcherbakova, D. M., Xia, J., Wang, L. V., Verkhusha, V. V., "Multicontrast photoacoustic in vivo imaging using near-infrared fluorescent proteins," Sci. Rep. **4**, 3939 (2014).

[7] Laufer, J., Zhang, E., Beard, P., "Evaluation of Absorbing Chromophores Used in Tissue Phantoms for Quantitative Photoacoustic Spectroscopy and Imaging," IEEE J. Sel. Top. Quantum Electron. **16**(3), 600–607 (2010).

[8] Laufer, J., Delpy, D., Elwell, C., Beard, P., "Quantitative spatially resolved measurement of tissue chromophore concentrations using photoacoustic spectroscopy: application to the measurement of blood oxygenation and haemoglobin concentration," Phys. Med. Biol. **52**(1), 141–168 (2007).

[9] Cox, B. T., Arridge, S. R., Beard, P. C., "Estimating chromophore distributions from multiwavelength photoacoustic images," J. Opt. Soc. Am. A, Opt. Image Sci. Vis. **26**(2), 443–455 (2009).

[10] Laufer, J., Jathoul, A., Pule, M., Beard, P., "In vitro characterization of genetically expressed absorbing proteins using photoacoustic spectroscopy," Biomed. Opt. Express **4**(11), 2477 (2013).

[11] Märk, J., Theiss, C., Schmitt, F.-J., Laufer, J., "Photoacoustic imaging of a near-infrared fluorescent marker based on dual wavelength pump-probe excitation," SPIE Proc. **8943**, A. A. Oraevsky and L. V. Wang, Eds., 894333 (2014).

[12] Märk, J., Schmitt, F., Laufer, J., "Photoacoustic imaging of the excited state lifetime of fluorophores," J. Opt. (in press).

[13] Märk, J., Schmitt, F.-J., Theiss, C., Dortay, H., Friedrich, T., Laufer, J., "Photoacoustic imaging of fluorophores using pump-probe excitation," Biomed. Opt. Express **6**(7), 2522–2535 (2015).

[14] Penzkofer, A., Falkenstein, W., Kaiser, W., "Vibronic relaxation in the S1 state of rhodamine dye solutions," Chem. Phys. Lett. **44**(1), 82–87 (1976).

[15] Jung, G., Wiehler, J., Zumbusch, A., "The photophysics of green fluorescent protein: influence of the key amino acids at positions 65, 203, and 222," Biophys. J. **88**(3), 1932–1947, Elsevier (2005).

[16] Hendrix, J., Flors, C., Dedecker, P., Hofkens, J., Y., "Dark states in monomeric red fluorescent proteins studied by fluorescence correlation and single molecule spectroscopy," Biophys. J. **94**(May) (2008).

[17] Penzkofer, A., Blau, W., "Theoretical analysis of S1-state lifetime measurements of dyes with picosecond laser pulses," Opt. Quantum Electron. **15**, 325–347 (1983).

[18] Grofcsik, A., Jones, W. J., "Stimulated Emission Cross-sections in Fluorescent Dye Solutions I Gain Spectra and Excited-state Lifetimes of Nile Blue A and Oxazine," J. Chem. Soc. Faraday Trans. **88**(8), 1101–1106 (1992).

[19] Min, W., Lu, S., Chong, S., Roy, R., Holtom, G. R., Xie, X. S., "Imaging chromophores with undetectable fluorescence by stimulated emission microscopy.," Nature **461**(7267), 1105–1109, Nature Publishing Group (2009).

[20] Zhang, E., Laufer, J., Beard, P., "Backward-mode multiwavelength photoacoustic scanner using a planar Fabry-Perot polymer film ultrasound sensor for high-resolution three-dimensional imaging of biological tissues," Appl. Opt. **47**(4), 561–577 (2008).